Assessment of groundwater potential zone mapping for semi-arid environment areas using AHP and MIF techniques

Sachin P. Shinde[1], Virendra N. Barai[1], Bhau K. Gavit[1], Sunil A. Kadam[2], Atul A. Atre[1], Chaitanya Baliram Pande[3], Subodh Chandra Pal[4], Neyara Radwan[5,6], Abebe Debele Tolche[7*] and Ismail Elkhrachy[8]

Abstract

Groundwater resources are essential for drinking water, irrigation, and the economy mainly in semiarid environments where rainfall is limited. Currently, unpredictable rainfall due to climate change and pollution on the Earth's surface directly affects groundwater resources. In this area, most people depend on groundwater resources for irrigation and drinking purposes, and every summer, most of the area depends on groundwater in a semiarid environment. Hence, we selected two popular methods, the analytical hierarchy process (AHP) and multiple influence factor (MIF) methods, which can be applied to map groundwater potential zones. Nine thematic layers, such as land use and land cover (LULC), geomorphology, soil, drainage density, slope, lineament density, elevation, groundwater level, and geology maps, were selected for this study using remote sensing and geographic information system (GIS) techniques. These layers are integrated in ArcGIS 10.5 software with the help of the AHP and MIF methods. The map of the groundwater potential zones in the study area revealed four classes, i.e., poor, moderate, good, and very good, based on the AHP and MF methods. The groundwater potential zone area is 241.50 (ha) Poor, 285.64 (ha) moderate, 408.31 (ha) good, and 92.75 (ha) very good using the AHP method. Similarly, the MIF method revealed that the groundwater potential classes were divided into four classes: 351.29 (ha) poor, 511.18 (ha), moderate, 123.95 (ha) good, and 41.78 (ha) very good. The results were compared to determine which methods are best for planning water and land resource development in specific areas that have basaltic rock and drought conditions. Both groundwater potential zone maps were validated with water yield data. The receiver operating characteristic (ROC) curve and area under the curve (AUC) model results are found to be 0.80 (good) and 0.93 (excellent) using the MIF and AHP methods, respectively; hence, the AHP method is best for delineation of groundwater potential zone maps and groundwater resource planning. The present study's framework and the results will be valuable for improving the efficiency of irrigation, conserving rainwater and maintaining the ecosystem in India.

Keywords MIF, AHP, Groundwater, ROC, Remote sensing

*Correspondence:
Abebe Debele Tolche
abeberobe@gmail.com
Full list of author information is available at the end of the article

Introduction

Groundwater is the subsequent largest contributor to fresh water on the planet. It is most important for economic and operational planning and implementation [1–3]. As a result of the progression of severe farming crossways to meet growing food and energy stresses worldwide [4–6], the overexploitation of groundwater has resulted in decreasing groundwater table [7] and an ever-accumulative pressure on accessible groundwater resources across many places around the world [8–11]. The groundwater supply is essential for crop and factory production [12]. The management of surface water is essential in the drought conditions of Maharashtra [13, 14].

The water is most important resource because it is naturally provides the most useful resources on the Earth's surface. With respect to the solution of life, the everyday actions and commercial expansion of some nations are unconditionally based on water resources [15–17]. Approximately 71% of the Earth's surface is enclosed by water bodies, constituting an enormous portion of the Earth's total area. However, the most common crushing water, approximately 96.5%, is saline water, which mainly includes oceans, seas, and bays [18–20]. The amount of freshwater utilized for domestic determination is only 3.5, and 68% of the freshwater available on the surface is obtained from glaciers, while 30% is confined under the surface or created from aquifer resources via groundwater, and the remaining 2% is observed in rivers, ponds, and the air [21–23]. Currently, nearly all studies agree that surface freshwater insufficiency is the greatest dangerous issue for all nations in the world [24–26]. This is due to a number of complex ecological difficulties, such as the undying deforestation that has caused severe climate variation and scarcity, the considerable daily surface and groundwater pollution caused by waste and discharge from rapidly prolonged manufacturing and urban expansion; and the increased demand for fundamentally amplified urban expansion and industries [27–29]. Therefore, these variables are powerful tools for an identifying other options for groundwater resources because of their demand and source [30].

Agriculture contributes significantly to the Indian economy. India has the second largest population in the world [31]. Groundwater potential zone mapping is required to establish groundwater and rainfall preservation strategies for semiarid regions, and whole planning is performed using remote sensing (RS) methods [32–34]. Basic and numerical datasets have been created by combining RS and geographic information system (GIS) data [35, 36]. RS has played a crucial role in natural resource mapping and analysis at regional scales [37]. A grouping of RS and GIS technology information is evaluated and used to designate and evaluate potential groundwater places [38]. RS and GIS are powerful tools for monitoring and managing groundwater resources at local and regional scales. In deficient aquifer zones in basaltic rock, these approaches and techniques have been used to detect acceptable zones for groundwater development [39]. It uses many important layers, i.e., geology, lineament, rainfall, NDVI, slope, land use, and soil types, to ensure accuracy and reduce human errors. Historically, suitable groundwater sites have been defined using multiple influence factor (MIF) and analytical hierarchy process (AHP) techniques [40–42]. RS, GIS, and hydrological information were clustered [43], and statistical methods were used [44]. New technologies such as MIF, AHP, RS, and GIS have correctly identified appropriate groundwater zones for planning and managing basins at local and global scales [42, 45]. RS and GIS are helpful for combining spatial and geophysical datasets for groundwater potential zone mapping [35]. Various approaches have been used to define appropriate sites for groundwater mapping based on the MIF and AHP methods [40, 46, 47]. Many researchers have used the AHP and MIF techniques to study groundwater potential zones with reference to RS and GIS datasets, therefore, these techniques provide precise valuations and decrease the probability of human mistakes [42]. Hence, the AHP and MIF methods have been used in hard rock study areas to create maps of suitable groundwater zones. This paper provides original and important results for the development of groundwater in hard rock areas with the help of the RS, GIS, MIF and AHP methods. In this work, all recent datasets were used to compare the MIF and AHP methods, which are the best for the mapping of groundwater potential zones in hard rock areas. Hence, large datasets of thematic layers are integrated to demarcate groundwater potential zones using a GIS system [48]. This work aimed to construct an accurate groundwater potential map based on GIS data and the MIF and AHP methods. The results are useful for the development of groundwater resources and land resource planning in the semi-arid environment and area of Maharashtra, India.

The main objectives of this study are as follows:

1. To create various thematic layers from satellite data and field verification information.
2. To identify the groundwater potential zone using the MIF and AHP methods.
3. To compare and validate groundwater potential zone maps and select the best methods for groundwater potential zone mapping in the semiarid environment.
4. To development the action plan map of land and water resources development plan for groundwater development in the semi-arid region of India.

Paper contribution

This paper main contribution lies in its application of two distinct methods, AHP and MIF, which have been used to generate groundwater potential zone maps in this region. This area is facing more challenges due to unpredictable rainfall caused by climate change and increasing population. By integrating the nine thematic layers derived from RS and GIS satellites, this study offers a comprehensive analysis of groundwater potential, considering various factors such as land use, geomorphology, soil, drainage density, slope, lineament density, elevation, groundwater level, and geology. The significance of this research is highlighted by its relevance to areas heavily reliant on groundwater for drinking, irrigation, and economic activities. Additionally, the study focuses on specific geological conditions, such as basaltic rock and drought conditions, making it applicable to regions facing similar hydrogeological challenges. Furthermore, the paper emphasizes the importance of exploring interdisciplinary collaborations and potential synergies with related research areas to enhance the scope and impact of the work. By engaging with experts from various fields, the research findings can be applied to address broader water resource management challenges and contribute to sustainable development. Overall, this paper's main contribution lies in providing valuable insights into groundwater potential assessment using two methods: satellite data integration techniques and popular methodologies. Both the methods were compared and the best method was selected for the development of groundwater potential zone maps in the semiarid region. The most powerful methods will be used for weighting various thematic layers in the GIS software. An important contribution of this paper is that the best and most important layers for the prediction of groundwater potential zones are mapped with increasing planning for groundwater development. The approach adopted in the study has the potential to improve water resource management practices, aid in groundwater planning, and support decision-making in regions facing water scarcity and environmental changes. The emphasis on interdisciplinary collaboration further underscores the significance of this research and its potential to influence policy-making and ecosystem preservation efforts in India and beyond.

Materials and methods

Study area

The Buchakewadi watershed is situated in the Junnar block of the Pune district in Maharashtra, India. The study area was between 19° 9′N and 19° 16′N latitude and 73° 47′E and 73° 64′E longitude. The location map is presented in Fig. 1. The watershed is demarcated by Survey of India (SOI) Topo-sheet No. E43B16 on a 1:50,000 scale. The observed average annual rainfall is 741.90 mm. Total study area is 1028.21 ha (10.28 km^2). The research area
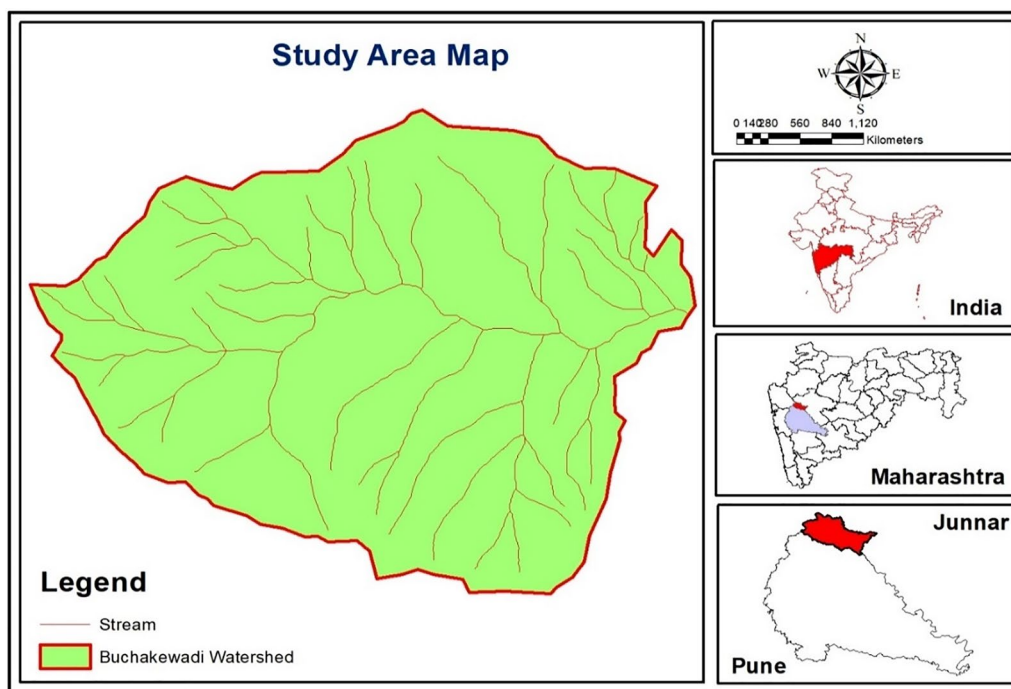

Fig. 1 Map of the study area

Shinde *et al. Environmental Sciences Europe*   (2024) 36:87

Page 4 of 20

is situated between the Western Ghats and the Deccan Plateau. In this area, Farmers have cultivated land for the entire three seasons. Hence this study area's most important work for the groundwater potential zones maps with day-by-day groundwater level decreasing in the last two decades, hence this reason this study has been selected for the preparation of thematics and groundwater maps. In the study area, most of the land is covered by agriculture and wasteland and some land under the forest area. In this view, groundwater suitable zones mapping should be most important for maintaining the ecosystem and groundwater depth throughout the entire study area.

Methodology

Groundwater potential zone mapping using traditional methods is very challenging. In the traditional approach, challenges arise due to the absence of thematic layers such as geomorphology, soil, and groundwater level data from reliable sources. Additionally, the lack of past maps or information from relevant departments and organizations further complicates the data collection process. This leads to difficulties in validating the accuracy and reliability of groundwater potential zone mapping. These challenges highlight the limitations and gaps in traditional methods for conducting such mapping exercises. Recently, the use of satellite data has become increasingly prevalent for creating thematic layers in various applications, including groundwater potential zone mapping. Satellite imagery provides valuable information about land cover, vegetation indices, and other relevant parameters. These satellite-derived thematic layers can serve as a starting point for analysing and assessing groundwater potential. However, it is important to note that field information is still crucial for final map creation, even when using advanced integrated methods. Field data collection helps validate and refine satellite-derived thematic layers, ensuring their accuracy and reliability. Field surveys provide ground truth information on various factors, such as lithology, soil characteristics, groundwater levels, and hydrological features, that cannot always be accurately captured through RS alone. The integration of satellite data with field information allows for a more comprehensive and robust groundwater potential zone mapping approach. This approach helps bridge the gap between RS observations and ground realities, improving the accuracy and reliability of the final map. Therefore, while satellite data play a vital role in the initial stages of mapping, field information remains essential for the validation and refinement of the results. A number of thematic layers, such as land use and land cover (LULC), geomorphology, soil, drainage density, slope, elevation, groundwater level, and geology, were prepared from satellite data [49]. We assigned the weights to nine thematic layers and integrated them into ArcGIS software 10.5. Basin-level geological and hydrological information is essential for spatial groundwater circulation. We compared the AHP and MIF methods based on nine thematic layers and ROC models. Water and soil data were collected from wells and farm plots via random sampling. Soil and water sample data were analysed at the Department of Soil Science, Mahatma Phule Krishi Vidyapeeth, Rahuri. Soil texture and groundwater depth maps were prepared based on field information using ArcGIS 10.5 software. The groundwater level data were helpful in the validation of groundwater potential zone maps using AUROC curves. The ROC is the most fundamental way to determine the dependability of an analytical assessment [50]. The accuracy of the two groundwater potential zones was determined by receiver operating characteristic (ROC) curves, which accurately delineate the groundwater potential zones. The best methods for mapping groundwater potential zones are the AHP and MIF methods (Fig. 2).

Multi-criteria decision analysis (MCDA) using the analytic hierarchy process (AHP)

Decision-making, for which we have collected most of our material, has become a scientific science. Psychological studies have shown that human beings make biases while making decisions. In view of these biases and the increasing complexity of present-day problems, there is a need for a methodology that is easy to comprehend and use for making effective and safe decisions [50, 51]. However, a methodology was required that could be used in a more natural way by decision-makers [52]. AHP satisfies all these requirements and has been adopted and used by many organizations worldwide for solving many decision-making problems. Saaty [53] created the analytic hierarchy process (AHP). This approach is a useful tool for resolving complex decision-making problems, and it can help policy makers set priorities and create suitable results. The AHP supports both subjective and objective features of a decision by dropping composite judgments to a sequence of pairwise comparisons and findings. Furthermore, the AHP is a practical method for examining the accuracy of decision-makers' assessments, thereby eliminating decision-making bias. Since the comparisons are made through subjective or personal perception, some amount of inconsistency may occur. To ensure that the perceptions are consistent, the consistency was verified by determining the consistency ratio, which is included to measure the degree of consistency among the pairwise comparisons of various criteria, which is considered one of the most significant advantages of the AHP. The AHP integrates and covers input in the form of spatial data to output in the form of decisions. The qualitative data of different themes and features are transformed into quantitative data by forming a pairwise comparison matrix using Saaty's scale [53–56]. The scale was
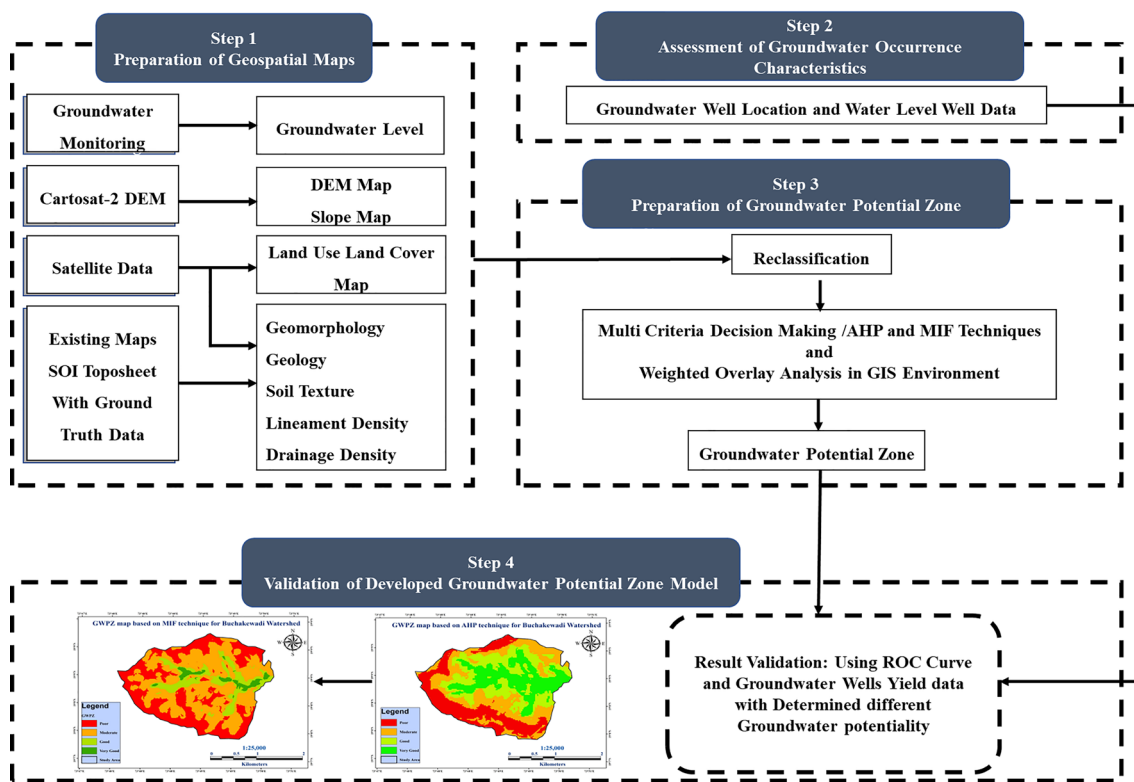
Fig. 2 Flowchart of the methodology

used to assign the judgement values provided (Table 1). The basic procedure consists of setting up the goal, considering and analysing the factors or criteria that affect the final decision and assigning judgement to different criteria using Saaty's scale (Tables 3, 4 and 5). To determine the consistency of the assigned weights, the consistency ratio (CR), as suggested by [53], was computed using Eqs. (1) and (2):

$$CR = \frac{CI}{RCI} \qquad (1)$$

where CI is consistency index and RCI is random consistency index.

The consistency index (CI) is given by Eq. (2):

$$CI = \frac{\lambda_{\max} - n}{n - 1} \qquad (2)$$

where λmax is the principal eigenvalue and n is the number of criteria. The random index is an estimation of the average value of the consistency index obtained from

Table 1 Scale for pairwise comparison [56]

Intensity of importance	Definition	Explanation
1.	Equal importance	Two activities contribute equally to the objective
2.	Equal to moderate importance	Experience and judgement slightly favour one activity over another
3.	Moderate importance	
4.	Moderate to strong importance	Experience and judgement strongly favour one activity over another
5.	Strong importance	
6.	Strong to very strong importance	An activity is favoured very strongly over another, its dominance demonstrated in practice
7.	Very strong importance	
8.	Very strong to extremely strong importance	The evidence favouring one activity over another is of the highest possible order of affirmation
9.	Extremely strong importance	

Shinde *et al. Environmental Sciences Europe*   (2024) 36:87

Page 6 of 20

large enough randomly generated matrices of size n (Table 2).

The computed value of the CR should be less than 10% to ensure consistency in decision-making; otherwise, the assigned weights should be re-evaluated to maintain consistency. If the CR is less than 10%, the judgements are consistent, which can be considered suitable for AHP analysis [54].

AHP analysis procedure

The detailed procedure for computing the weights of the criterion is presented below:

Form a pairwise comparison matrix given as Eq. (3):

$$\begin{bmatrix} C11 & C12 & C13 \\ C21 & C22 & C23 \\ C31 & C32 & C33 \end{bmatrix} \tag{3}$$

The sum of the values of each column of the pairwise comparison matrix is given as Eq. (4):

$$SC_{ij} = \sum_{i=1}^{n} C_{ij} \tag{4}$$

A normalized comparison matrix is calculated by dividing each entry in a column by its column total Eqs. (5 and 6):

$$X_{ij} = \frac{C_{ij}}{\sum_{i=1}^{n} C_{ij}} = \begin{bmatrix} X11 & X12 & X13 \\ X21 & X22 & X23 \\ X31 & X32 & X33 \end{bmatrix} \tag{5}$$

where

$$C_{ij} = \begin{bmatrix} C11 & C12 & C13 \\ C21 & C22 & C23 \\ C31 & C32 & C33 \end{bmatrix} \tag{6}$$

The sum of each row is computed and divided by the number of criteria to obtain the criteria weights, as shown in Eq. (7):

$$W_{ij} = \frac{\sum_{i=1}^{n} C_{ij}}{n} = \begin{bmatrix} W11 \\ W12 \\ W13 \end{bmatrix} \tag{7}$$

Multiply the criterion weights obtained with the original pairwise comparison matrix to get the weighted sum value. Divide the weighted sum value with the corresponding criterion weight to get the consistency vector as, Eqs. (8 to 11):

$$\begin{bmatrix} C11 & C12 & C13 \\ C21 & C22 & C23 \\ C31 & C32 & C33 \end{bmatrix} \times \begin{bmatrix} W11 \\ W21 \\ W31 \end{bmatrix} = \begin{bmatrix} C_{V11} \\ C_{V21} \\ C_{V31} \end{bmatrix} \tag{8}$$

This is obtained by

$$C_{V11} = \frac{1}{W_{11}}[C_{11}\ W_{11} + C_{12}\ W_{21} + C_{13}\ W_{31}] \tag{9}$$

$$C_{V21} = \frac{1}{W_{21}}[C_{21}\ W_{11} + C_{22}\ W_{21} + C_{23}\ W_{31}] \tag{10}$$

$$C_{V31} = \frac{1}{W_{31}}[C_{31}\ W_{11} + C_{32}\ W_{21} + C_{33}\ W_{31}] \tag{11}$$

The value of λmax was determined by averaging the values of the consistency vector (Eq. 12):

$$\lambda = \sum_{i=1}^{n} C_{Vij} \tag{12}$$

- Find the consistency index.
- Select the value of random consistency index from Table 6 based on number of criteria.
- Finally compute the consistency ratio using the equation.
- If the consistency ratio < 0.10, then our judgements are consistent and there is no biasness in our decision-making. If it is more than 0.10, then repeat the procedure again by altering comparison values in pairwise comparison matrix.

The key objectives are to define the groundwater potential zones. Nine different criteria, namely, geomorphology, geology, soil, slope, elevation, drainage density, lineament density, land use/land cover and groundwater level, were selected for this AHP analysis. Each of these criteria have subcriteria, e.g., land use consisted of forest, cropland, scrubland, water bodies and built-up areas. First, ranks were given to the subcriteria, and then the main criterion was determined using Saaty's scale from 1 to 9 to form a pairwise comparison matrix; subsequently, the weights were finalized (Tables 3, 4, 5, 6, 7, 8, 9, 10).

Table 2 The values of RCI for different order of matrix

No. of criteria	1	2	3	4	5	6	7	8	9	10
RCI	0	0	0.58	0.9	1.12	1.24	1.32	1.41	1.45	1.51

Table 3 Continuous rating scale of Satty's analytical hierarchical process

1/9	1/7	1/5	1/3	1	3	5	7	9
Extremely	Very strong	Strongly	Moderately	Equally	Moderately	Strongly	Very strong	Extremely
Less important ⬅️━━━━				Equally	━━━━➡️ More important			

Multi-influencing factors of groundwater potential zones

Table 11 shows the main components that illustrate the interrelationships between these parameters and their impacts. Each relationship is divided into major and small impacts and weighted based on its strength in the diagram. A score of 1.0 was assigned if a major effect was observed, indicating a strong link between factors. If a minor effect occurred, indicating poor parameter relationships, those parameters were given a score of 0.5 [57]. The cumulative weight of major and minor influences was used to compute the comparison score for every element to potential groundwater zones [58]. This comparative score can also be used to calculate the expected score of each independently affected factor, as presented in Eq. (13). The relationships among the interparameters of the multiple influencing factors are shown in Fig. 3:

$$D = \left(\frac{(A + B)}{\sum (A + B)} \right) \times 100 \tag{13}$$

where D means the future score of each influencing factor, a positions for the major interrelationship with both factors, and B stands for the minor interrelationship with two parameters. Each group of the single themes are provided a position during weighted overlay study. In accordance with groundwater hydrogeology, the required scores have assigned in accordance with the multi-influencing factor (MIF) of specific element [42, 57].

Sensitivity analysis

The present work has accepted map exclusion and individual factor sensitivity analysis approaches to appreciate the influential thematic layers of the determined groundwater potential zones and the inspiration of the given weights and rank to every class and subclasses and thematic map.

Model validation for potential groundwater zones

For the definition of groundwater potential zones, two types of approaches were used in this study: AHP and MIF. These techniques provided more precise information about groundwater suitability in semiarid and dry regions. The potential groundwater zone outcome maps were evaluated using existing groundwater level data. The water level data were acquired from open well locations and mapped over the entire watershed area's probable groundwater zones. The ROC curve and area under the curve (AUC) were used to determine which approaches were appropriate for mapping suitable groundwater zones mapping to acquire the correctness of the potential zones of groundwater maps [59, 60]. The development of groundwater resources can be aided by these groundwater potential zone maps. The region under the ROC curve in the ROC system ranges between 0.5 and 1.0. It is utilized to determine how accurate the model is. The models do not describe the presence of a groundwater zone, and the AUC is equal to 0.5. The true positive (sensitivity) and false-positive (1-specificity) rates are shown on the Y and X axes, respectively, to provide a graphical depiction of the ROC curve [61]. This study used a total of 113 sites to determine the depth of the groundwater table.

Accuracy assessment Potential zones of groundwater maps were created and validated and compared to the groundwater depth data collected from the well location during the field survey. The observation wells are overlaid on the groundwater potential zone maps generated via the MIF and AHP methods, which are highly accurate for determining the results via Eq. (14):

$$\text{Accuracy of high GWP (\%)}$$
$$= \frac{\text{Well with low GWF in high GWPZ}}{\text{Total no. of wells in low GWP}} \times 100 \tag{14}$$

Results and discussion
Thematic layers

The nine thematic layers are used to delineate groundwater potential zone maps with the help of the AHP and MIF methods. The thematic layers are described in detail below.

Geology

The determination of groundwater potential zones, as well as their analysis and occurrence, is supported by geology. Groundwater and dry spells are major issues throughout the entire region, especially in semiarid areas. Basaltic rock is found in the area (Fig. 4).

Table 4 Assigned weights of different features of all the thematic maps

S. No.	Influencing factors	Class interval	Groundwater availability	Saaty's scale (in Frac.)	Saaty's scale (in Deci.)	% Influence = (Saaty's scale/sum) * 100	Relative weight
1	Drainage density	0–7.5 km/km^2	Very high	1	1	46.08	46
		7.5–15.02 km/km^2	High	1/2	0.5	23.04	23
		15.02–22.53 km/km^2	Moderate	1/3	0.33	15.20	15
		22.53–30.05 km/km^2	Low	1/5	0.2	9.2	9
		30.05–37.56 km/km^2	Very low	1/7	0.14	6.4	7
		Total			2.17	100	
2	Geology	Deccan trap	Moderate	1/3	0.33	100	100
		Total			0.33	100	
3	Geomorphology	Weathered canal command	Very high	1	1	40.32	40
		Weathered	High	1/2	0.5	20.16	20
		Undissected	Moderate	1/3	0.33	13.30	14
		Slightly dissected	Moderate	1/4	0.25	10.08	10
		Moderately dissected	Moderate	1/5	0.2	8.06	8
		Highly dissected	Low	1/5	0.2	8.06	8
		Total			2.48	100	
4	Land use land cover	Water body	Very high	1	1	46.08	46
		Forest	High	1/2	0.5	23.04	23
		Agriculture land	Moderate	1/3	0.33	15.20	15
		Waste land	Low	1/5	0.2	9.2	9
		Built up	Very low	1/7	0.14	6.4	7
		Total			2.17	100	
5	Soil texture	Clay	Very high	1	1	49.26	49
		Clay loam	High	1/2	0.5	24.63	25
		Sandy clay loam	Moderate	1/3	0.33	16.25	16
		Sandy loam	Low	1/5	0.2	9.8	10
		Total			2.03	100	
6	Slope	0–1%	Very high	1	1	38.31	38
		1–3%	High	1/2	0.5	19.15	19
		3–5%	Moderate	1/3	0.33	12.64	12
		5–10%	Moderate	1/3	0.33	12.64	12
		10–15%	Low	1/5	0.2	7.66	8
		15–35%	Very low	1/7	0.14	5.36	6
		>35%	Extreme low	1/9	0.11	4.21	5
		Total			2.61	100	
7	Lineament density	5–2.5 km/km^2	Very high	1	1	46.08	46
		2.5–1.5 km/km^2	High	1/2	0.5	23.04	23
		1.5–1 km/km^2	Moderate	1/3	0.33	15.20	15
		1–0.5 km/km^2	Low	1/5	0.2	9.21	9
		0.5–0 km/km^2	Very low	1/7	0.14	6.45	7
		Total			2.17	100	
8	Water level depth	0–3 m	Very high	1	1	46.08	46
		3–4 m	High	1/2	0.5	23.04	23
		4–5 m	Moderate	1/3	0.33	15.20	15
		5–6 m	Low	1/5	0.2	9.21	9
		6–8 m	Very low	1/7	0.14	6.45	7
		Total			2.17	100	

Table 4 (continued)

S. No.	Influencing factors	Class interval	Groundwater availability	Saaty's scale (in Frac.)	Saaty's scale (in Deci.)	% Influence = (Saaty's scale/sum) * 100	Relative weight
9	Elevation	700–800 m	Very high	1	1	46.08	46
		800–900 m	High	½	0.5	23.04	23
		900–1000 m	Moderate	1/3	0.33	15.20	15
		1000–1100 m	Low	1/5	0.2	9.21	9
		1100–1200 m	Very low	1/7	0.14	6.45	7
		Total			2.17	100	

Table 5 Pairwise comparison matrix of thematic layers

Layer	LULC	Geomorphology	Soil	Drainage density	Slope	Lineament density	Elevation	Ground water level	Geology
LULC	1	2	3	5	5	7	7	8	9
Geomorphology	1/2	1	2	3	5	7	7	9	9
Soil	1/3	1/2	1	2	3	5	7	7	9
Drainage density	1/5	1/3	1/2	1	2	3	5	5	7
Slope	1/5	1/5	1/3	1/2	1	2	3	5	7
Lineament density	1/7	1/7	1/5	1/3	1/2	1	2	3	5
Elevation	1/7	1/7	1/7	1/5	1/3	1/2	1	2	3
Ground water level	1/8	1/9	1/7	1/5	1/5	1/3	1/2	1	2
Geology	1/9	1/9	1/9	1/7	1/7	1/5	1/3	1/2	1
Total	2.76	4.54	7.43	12.38	17.18	26.03	32.83	40.50	52.00

Table 6 Random index (RI) values for the number of thematic layers (*n*)

n	1	2	3	4	5	6	7	8	9	10
RI	0	0	0.58	0.9	1.12	1.24	1.32	1.41	1.45	1.51

Table 7 Normalized matrix

LULC	Geomorphology	Soil texture	Drainage density	Slope	Lineament density	Elevation	Ground water level	Geology	Total	Eigen vector (average)
0.36	0.44	0.40	0.40	0.29	0.27	0.21	0.20	0.17	2.75	0.31
0.18	0.22	0.27	0.24	0.29	0.27	0.21	0.22	0.17	2.08	0.23
0.12	0.11	0.13	0.16	0.17	0.19	0.21	0.17	0.17	1.45	0.16
0.07	0.07	0.07	0.08	0.12	0.12	0.15	0.12	0.13	0.94	0.10
0.07	0.04	0.04	0.04	0.06	0.08	0.09	0.12	0.13	0.69	0.08
0.05	0.03	0.03	0.03	0.03	0.04	0.06	0.07	0.10	0.44	0.05
0.05	0.03	0.02	0.02	0.02	0.02	0.03	0.05	0.06	0.29	0.03
0.05	0.02	0.02	0.02	0.01	0.01	0.02	0.02	0.04	0.21	0.02
0.04	0.02	0.01	0.01	0.01	0.01	0.01	0.01	0.02	0.15	0.02
(Total) 1.00	1.00	1.00	1.00	1.00	1.00	1.00	1.00	1.00	9	1.00

Table 8 Consistency measures

Layer	LULC	Geomorphology	Soil texture	Drainage density	Slope	Lineament density	Elevation	Ground water level	Geology	Total	Consistency measures	Consistency measures
LULC	1.00×0.31	2.00×0.23	3.00×0.16	5.00×0.10	5.00×0.08	7.00×0.05	7.00×0.03	8.00×0.02	9.00×0.02	3.16	3.16/0.31	9.93
Geomorphology	0.50×0.31	1.00×0.23	2.00×0.16	3.00×0.10	5.00×0.08	7.00×0.05	7.00×0.03	9.00×0.02	9.00×0.02	1.73	1.73/0.23	9.80
Soil texture	0.33×0.31	0.50×0.23	1.00×0.16	2.00×0.10	3.00×0.08	5.00×0.05	7.00×0.03	7.00×0.02	9.00×0.02	1.60	1.60/0.16	9.25
Drainage density	0.20×0.31	0.33×0.23	0.50×0.16	1.00×0.10	2.00×0.08	3.00×0.05	5.00×0.03	5.00×0.02	7.00×0.02	1.02	1.02/0.10	9.14
Slope	0.20×0.31	0.20×0.23	0.33×0.16	0.50×0.10	1.00×0.08	2.00×0.05	3.00×0.03	5.00×0.02	7.00×0.02	0.75	0.75/0.08	8.91
Lineament density	0.14×0.31	0.14×0.23	0.20×0.16	0.33×0.10	0.50×0.08	1.00×0.05	2.00×0.03	3.00×0.02	5.00×0.02	0.51	0.51/0.05	8.96
Elevation	0.14×0.31	0.14×0.23	0.14×0.16	0.20×0.10	0.33×0.08	0.50×0.05	1.00×0.03	2.00×0.02	3.00×0.02	0.31	0.31/0.03	8.91
Ground water level	0.13×0.31	0.11×0.23	0.14×0.16	0.20×0.10	0.20×0.08	0.33×0.05	0.50×0.03	1.00×0.02	2.00×0.02	0.24	0.24/0.02	9.17
Geology	0.11×0.31	0.11×0.23	0.11×0.16	0.14×0.10	0.14×0.08	0.20×0.05	0.33×0.03	0.50×0.02	1.00×0.02	0.16	0.16/0.02	9.27
Total												83.34

Table 9 Parameters (AHP) used to check the consistency of the matrix

AHP parameters	Formula	Values	Remarks
Consistency measures	$\frac{\text{(Row of comparison matrix)} \times \text{(eigen vector)}}{\text{Corresponding eigen vector of the row}}$	Table 8	Last column of the consistency table
Principal Eigen value	$\lambda_{\max}$	9.26	Average of the column of consistency measures
Consistency index (CI)	$\frac{\lambda_{\max} - n}{n-1}$	0.0325	n is number of thematic layers equal to 9 ($n = 9$)
Consistency ratio (CR)	$\frac{CI}{RI}$	0.022	RI is random index equal to 1.45 from Table 6 ($n = 9$)

Table 10 Weights for thematic layers using the AHP method

S. No.	Influencing factor	Value	Eigen Value	% Weightage
1	Land use land cover	High	0.31	31
2	Geomorphology		0.23	23
3	Soil texture		0.16	16
4	Drainage density		0.10	10
5	Slope		0.08	08
6	Lineament density		0.05	05
7	Elevation		0.03	03
8	Water level depth		0.02	02
9	Geology	Low	0.02	02
Total				100

Geomorphology

Geomorphological characteristics are important parameters for the conservation of rainwater in aquifers. In this view, geomorphology maps are important for groundwater development in the area. A geomorphological landform was found from satellite data using visual interpretations with reference to field data and Survey of India Topo-sheet maps [62, 63]. As a consequence, geomorphological mapping plays a vital role in identifying suitable groundwater zones and watershed conservation strategies. The geomorphology map in Fig. 4 shows the various land forms.

Slope It is a vital parameter factor for measuring prospective groundwater zones. It affects the total amount of surface water that infiltrates. Lower and greater values of the slope angle indicate thinner and sharper topography. Slope values between 3 and 50% are found in the study area. The slope map is presented in Fig. 4.

Drainage density

It is a vital factor in mapping potential groundwater zones, so many soil and water conservation activities have been performed on drainage lines and farmlands. The normalized weights of the Dd data layer were multiplied by the normalized weights of the separate elements presented in Table 4 to obtain the final weights of the drainage density layers (Fig. 4).

Land use/land cover

Sentinel-2 satellite data were used to construct the LULC map, which was generated using ArcGIS 10.5 software. Groundwater, drought, and agriculture areas are needed to planning of ecosystem and land use classes in dry or basaltic hard rock areas. The LULC map was created based on the satellite data and ground data. This water area LU/LC is classified into five classes: water body, forest, agriculture, waste, and built-up land. The LULC map is presented in Fig. 4.

Table 11 Proposed score of every influencing parameter

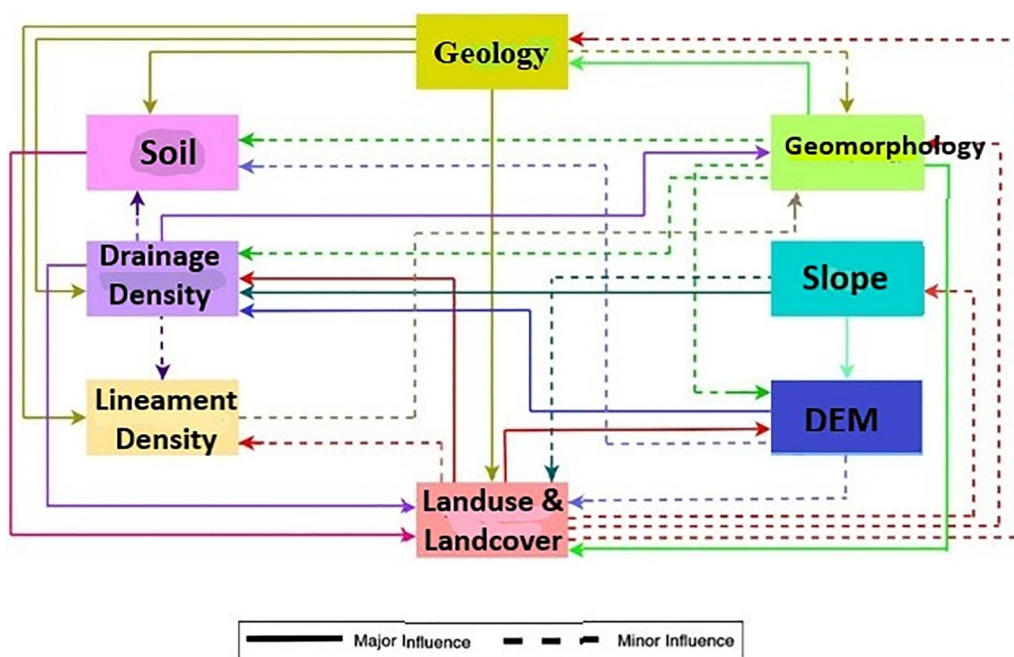| Factors	Major effect (A)	Minor effect (B)	Relative weight ($A + B$)	Assigned weight for each influential factor
Soil texture	3	0.5	3.5	19
Geomorphology	2	0.5	2.5	13
LULC	3	0	3	16
Lineament density	2	0.5	2.5	13
Slope	2	0	2	11
Drainage density	2	0	2	11
Elevation	1	0.5	1.5	8
Groundwater depth	1	0	1	6
Geology	0	0.5	0.5	2

Fig. 3 Relationship of the interparameters between the multiple influencing factors

Soil texture

The main aspect of determining potential groundwater zones is the soil. Several methods and technologies, such GIS, MIF, and AHP modelling, are currently used in groundwater research and water resources planning. Therefore, four such as clay, clay loam, sandy clay loam, sandy loam classes of soil are depicted in Fig. 4.

Lineament density

The irregular earth formations observed are lineaments and faults. These qualities revealed the surface and concealed layer properties. It is assumed that a high lineament density aids in the formation of the aquifer zone in hard basaltic rock with steep topography. The lineament depicts poor aquifer areas throughout the watershed. These data can be used to monitor groundwater growth and management to improve crops during the dry spell and winter seasons [64]. The lineament density map is shown in Fig. 4.

Water level depth

It is below the surface of the earth with saturated freshwater at which rainwater in a compressed aquifer would rise in volume. The most important aspect to use in preparation of possible groundwater locations is water level valuation. The water level depth map is shown in Fig. 4.

Elevation

The elevation layer was developed from CARTOSAT-30 m using spatial analysis tools and the elevation fluctuated from 700 to 1200 m (mean sea level) in the study area (Fig. 4).

Identification of groundwater potential zones using AHP and MIF methods

AHP method

Thomas L. Saaty established the AHP method to organize and analyse complex decisions mathematically using quantitative and qualitative data. It provides a framework for decision-making and addresses integrated GIS spatial analysis. The overall determination of the AHP can help decision-makers select the finest alternative from numerous probable replacements. It builds hierarchies to solve problems that allow for the calculation of the input by separate criteria at lower stages made to criteria at higher stages of hierarchy. It is an eigenvalue method to the pairwise evaluation method and affords a fundamental arithmetical scale (ranging from 1 to 9) to standardize the measurable and qualitative representations of priorities.

Analytic hierarchical process (AHP)-assigned weights for thematic maps   As discussed in the previous sections, various thematic features are studied for groundwater occurrence and control in the Buchakewadi watershed.
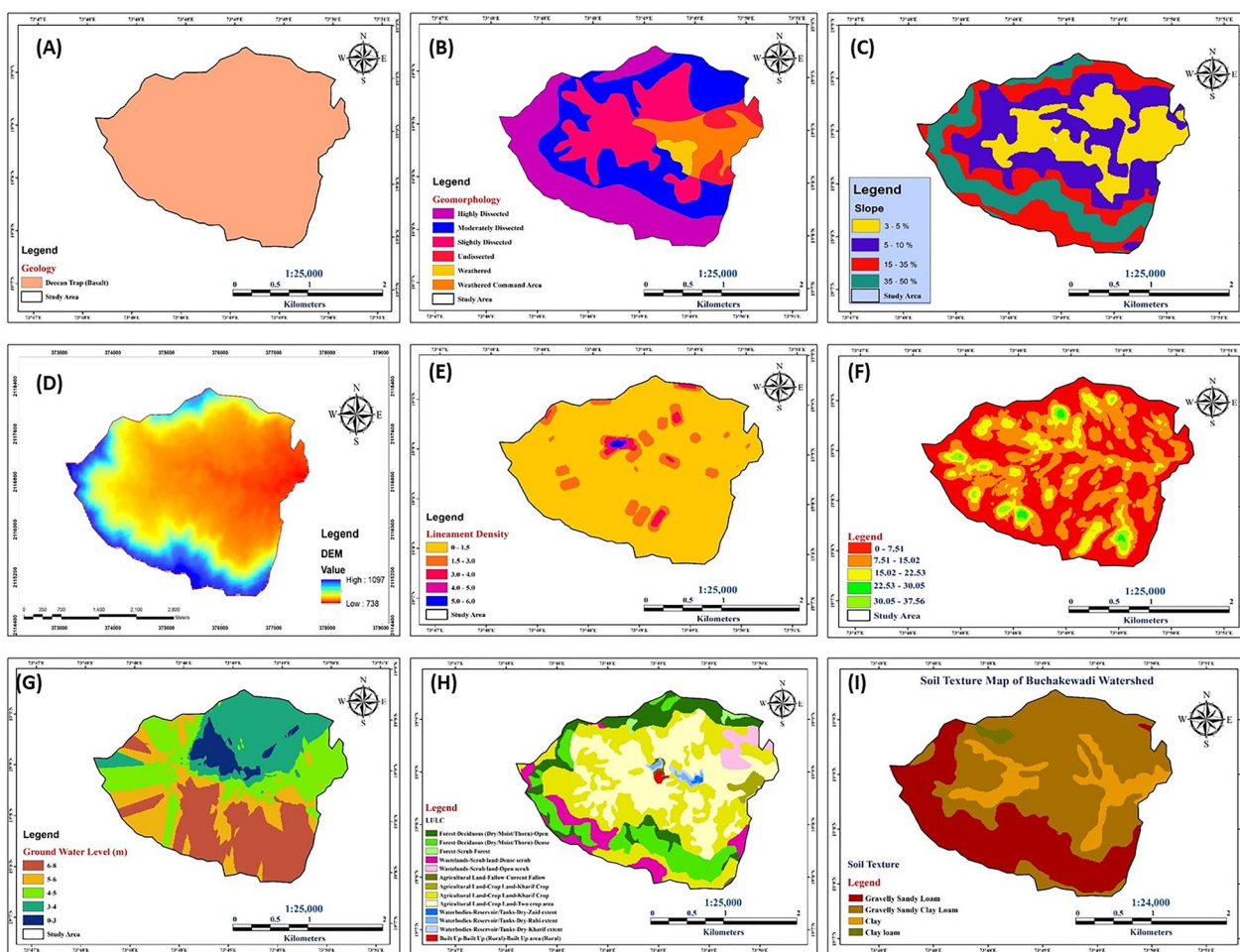
Fig. 4 Thematic layer maps of the study area: **A** geology, **B** geomorphology, **C** slope, **D** elevation, **E** lineament density, **F** drainage density, **G** groundwater level, **H** LULC, and **I** soil texture

The AHP was used to detect potential groundwater zones in the area. Taken together, thematic maps were assigned suitable weights for potential zones, and the groundwater development continuous rating scale of Saaty's AHP (Table 3) was used to assign weights to the individual features of each theme for each area. The weights assigned to each thematic map of the study area are tabulated in Table 4.

Weight assignment and normalization of thematic layers: Pairwise comparison of thematic layers   A matrix of pairwise comparisons of whole thematic layer factors was calculated in a square matrix, where the diagonal features of the matrix were constantly 1 (Table 5). These included thematic maps for geomorphology, slope, elevation, groundwater level, geology, etc. Thus, a 9×9 comparison matrix was formed, and factors of relative importance between the thematic layers were chosen from the pairwise comparison matrix rating scale

(Table 6). According to the protocol followed by [43], the lower triangular matrix was constructed by enchanting reciprocals of the corresponding importance factor of the upper triangular matrix (Eq. 15).

The pairwise comparison matrix $F(n)$ of Table 5

$$F(n) = \begin{pmatrix} 1 & 2 & 3 & 5 & 5 & 7 & 7 & 8 & 9 \\ 1/2 & 1 & 2 & 3 & 5 & 7 & 7 & 9 & 9 \\ 1/3 & 1/2 & 1 & 2 & 3 & 5 & 7 & 7 & 9 \\ 1/5 & 1/3 & 1/2 & 1 & 2 & 3 & 5 & 5 & 7 \\ 1/5 & 1/5 & 1/3 & 1/2 & 1 & 2 & 3 & 5 & 7 \\ 1/7 & 1/7 & 1/5 & 1/3 & 1/2 & 1 & 2 & 3 & 5 \\ 1/7 & 1/7 & 1/7 & 1/5 & 1/3 & 1/2 & 1 & 2 & 3 \\ 1/8 & 1/9 & 1/7 & 1/5 & 1/5 & 1/3 & 1/2 & 1 & 2 \\ 1/9 & 1/9 & 1/9 & 1/7 & 1/7 & 1/5 & 1/3 & 1/2 & 1 \end{pmatrix}.$$

(15)

The normalized matrix for the present study was obtained from the pairwise comparison matrix. The sum of the normalized records in every column should be one. The eigenvector is calculated as the average

Shinde *et al. Environmental Sciences Europe*   (2024) 36:87

Page 14 of 20

of all components in the row. The derived normalized matrix for the present study is presented in Table 7.

The consistency of the matrix is ensured. The matrix is considered consistent if all the elements have been obtained from the minimal amount of its elements. Moreover, the elements of the columns and rows of a consistent matrix will be proportional. The consistency measures used for the present study are presented in Table 8. The parameters used to determine the consistency of the normalized matrix via the AHP method are presented in Table 6 and Eq. (15).

Consistency ratio (CR) was computed using Eq. (1). CI is the consistency index and the term (*n*) is a random index that is completely based on the value of *n*. The values of RI (*n*) for $n \leq 10$ are listed in Table 9.

A consistency ratio (CR) less than or equal to 0.10 (0.022 < 0.10) is acceptable and implies that the matrix is consistent. The consistency ratio (CR) of the weights assigned to dissimilar thematic maps of the study area is 0.022, which implies that the matrix is consistent. A pairwise comparison of the thematic layers based on the criterion using Saaty's AHP was used to compute normalized weights for separate themes, as shown in Table 10. The highest weight was assigned to land use/ land cover (31%), followed by geomorphology (23%) and soil texture (16%). All of these weightages were measured by Eqs. (16) and (17).

Groundwater potential zones = (land use/land cover)

$\times$ (31) + (geomorphology) $\times$ (23) + (soil texture)

$\times$ (16) + (drainage density) $\times$ (10) + (slope) $\times$ (08)

+ (lineament density) $\times$ (05) + (elevation) $\times$ (03)

+ (water level depth) $\times$ (02) + (geology) $\times$ (02)

$$(16)$$

$$\text{Eigenvalue} = \frac{\text{Sum of all layers}}{\text{No. of layers}} \tag{17}$$

Overlay analysis

Overlay analysis was performed using the tool 'Weighted Overlay' in Overlay Toolset, which works within Spatial Analyst Tools in ArcGIS 10.5. The weighted overlay apparatus overlays various rasters utilizing a typical estimation scale and loads per its importance (ESRI). The resulting map obtained from the overlay analysis was classified into four classes: poor, moderate, good, and very good groundwater potential, as presented in Fig. 5. Using the AHP method, it was found that the Buchakewadi watershed contained 92.75 ha (9.02%) of very good territory, 408.31 ha (39.71%) of good territory, 285.64 ha (27.78%) of moderate territory, and 241.50 ha (23.48%) of poor groundwater potential.

MIF method

To identify potential groundwater zones in the Buchakewadi watershed, nine thematic parameters and subclasses were assigned weights to groundwater prospect maps via the MIF method [48]. The multi-influencing factor method is used to evaluate the impact of various parameters, and the weights given to every factor are calculated statistically. The elevation, geology, geomorphology, etc., are important parameters that influence groundwater potential recharge zone maps. Thematic layers are considered influencing factors for potential groundwater zones. The MIF technique is used to recognize potential groundwater zones. The major factor had a weight of 1.0, and the minor factor had a weight of 0.5. The cumulative weight of major and minor factors is considered for computing the comparative rates. This was then used to compute the score of every influential factor. The score of each influential factor was computed by Eq. (18):

$$\left[\frac{A+B}{\sum (A+B)} \right] * 100 \tag{18}$$

The proposed score for each influential factor influencing the groundwater potential in the Buchakewadi watershed area is shown in Table 11. After assigning weights and rates of elements and subclasses through the MIF technique, the influential thematic map layers were combined in ArcGIS 10.5 using the weighted overlay method [65]. The overlay map for the potential groundwater zones is presented in Fig. 5. The weighting details assigned to the different thematic layers and their characteristics are shown in Table 4. The proposed score of the separate influencing factors was separated and assigned to each reclassified subparameter. In the ArcGIS 10.5 platform, to analyse the GWP area, all these variables with their potential weights were merged into the GIS environment by applying a weighted overlay analysis. We have been found that groundwater potetnial zones classes such as poor (351.29 ha), moderate (511.18 ha), good (123.95 ha), very good (41.78 ha) using the MIF method [66].

Groundwater potential zone map validaton
Ground truth verification and validation

The groundwater potential zone maps were prepared using AHP, MIF and geospatial techniques (Fig. 5) and were verified and validated using village census data from wells in the Buchakewadi watershed, Junnar cluster, Pune, and Maharashtra. The number of wells in the groundwater potential zone identified using the AHP method is the highest and falls under very good groundwater potential. Similarly, a significantly high
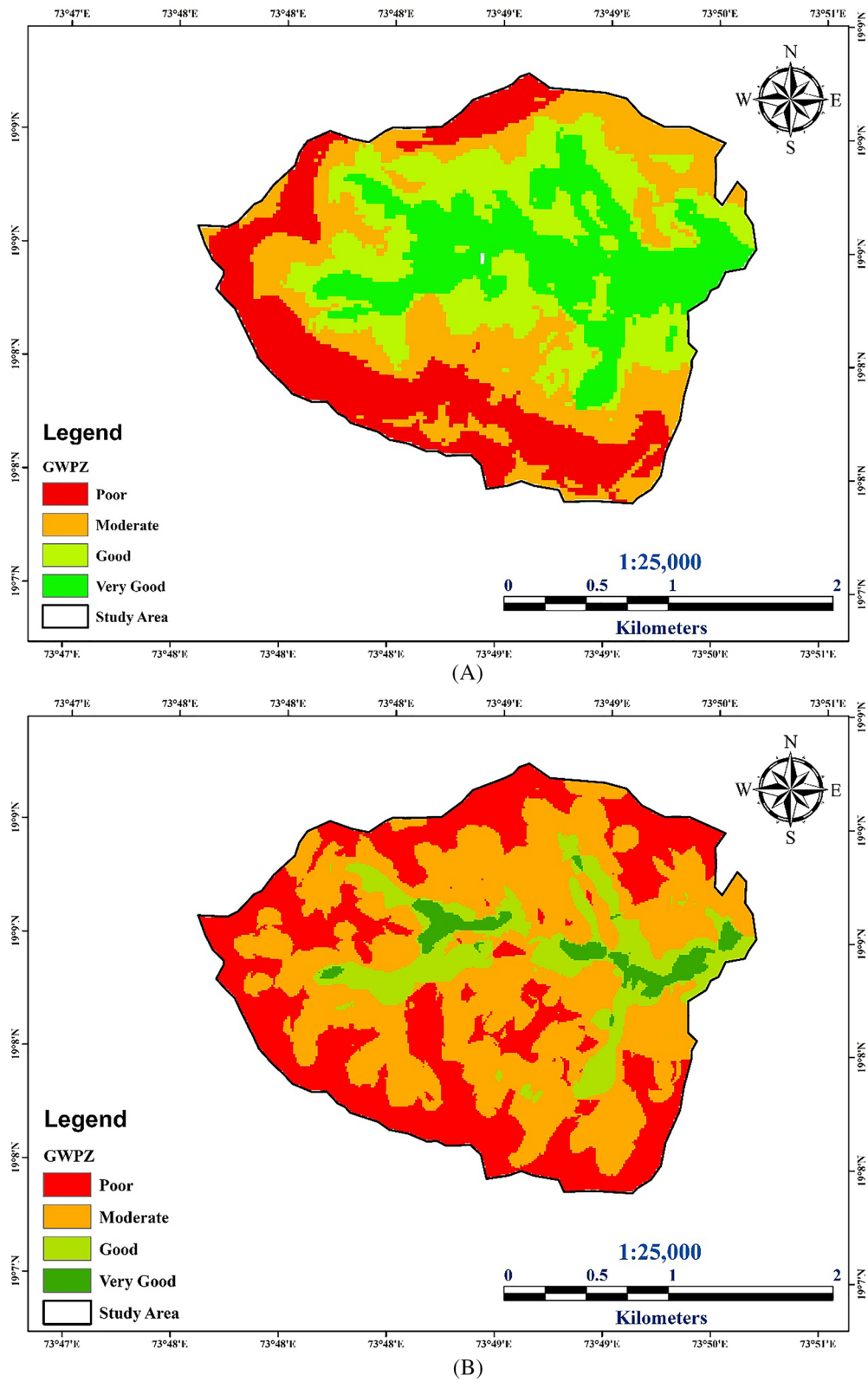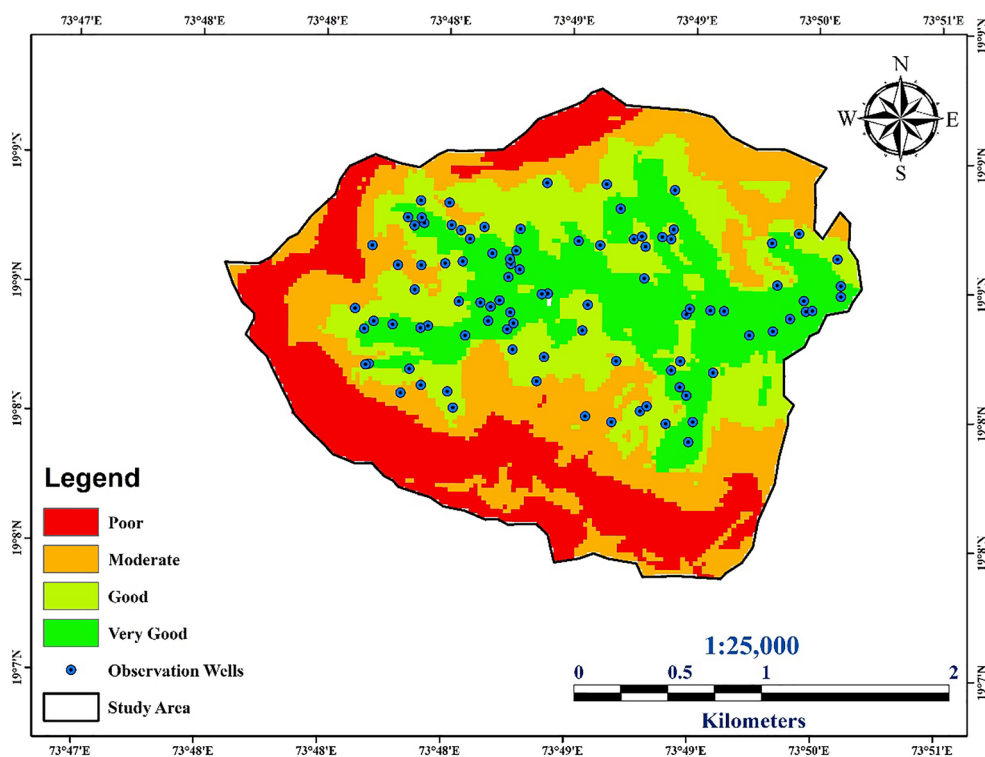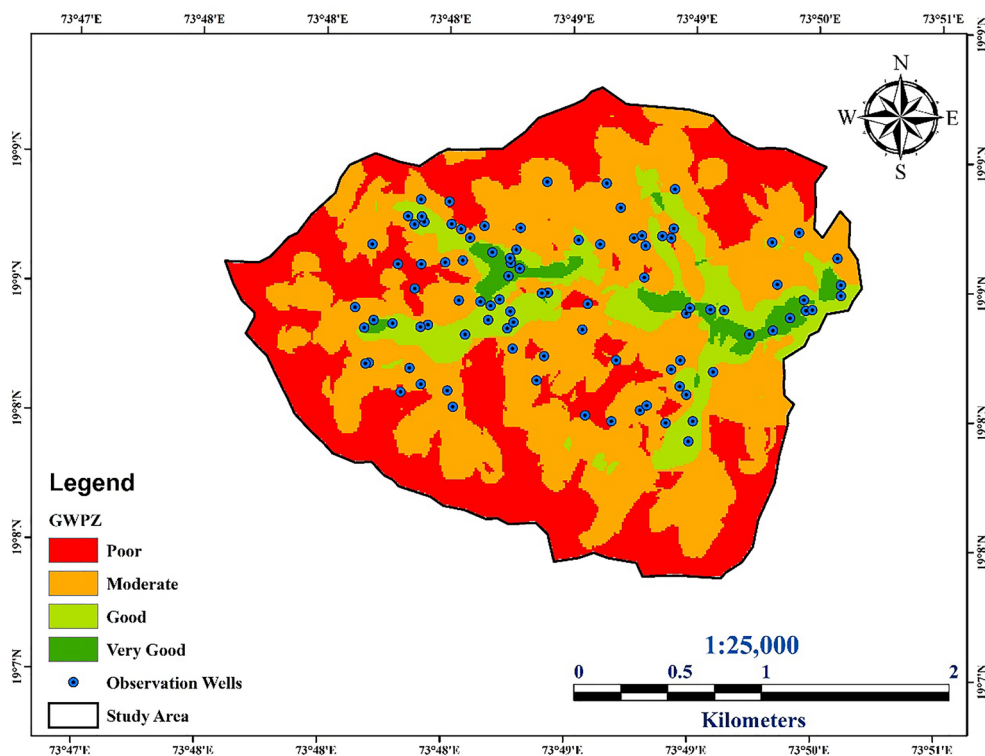
Fig. 5 Results of the groundwater potential zone map: **A** groundwater potential zone map using AHP, **B** groundwater potential zone map using MIF, **C** validated groundwater potential zone map of AHP, **D** validated groundwater potential zone map of MIF

(C)

(D)

Fig. 5 continued

number of wells fall under the groundwater potential zone identified using the MIF method. Thus, it has been concluded that the results obtained from the study are true compared to actual field data.

Validation of groundwater potential zone maps using AUROC curves

The AUROC curve was used to validate the groundwater potential zone maps using the AHP and MIF methods. It is used to assess the performance of multiclass classification problems. The ROC is the probability curve, and the AUC denotes the degree of reparability. The AUC values indicate the ability of a predicted model to distinguish between classes (Table 12). Thus, the higher the AUC is, the better the model predicts 0 classes as 0 and 1 classes as 1. The different groundwater potential zones and their area distributions identified using the AHP and MIF methods are shown in Table 12. The ROC curves for the groundwater potential maps derived using the AHP

and MIF methods are depicted in Figs. 6 and 7. The AUC for the model derived using AHP was 0.93, whereas for the MIF-derived model, it was 0.80 (Figs. 6 and 7). Thus, the groundwater potential zones identified using both methods are valid, with the AHP-derived zones having a higher probability of success.

Conclusions

The research focused on identifying potential groundwater zones in an entire watershed area using the MIF and AHP methods. The study aimed to assess groundwater recharge sites and delineate prospective zones in basaltic rock formations, which are crucial for long-term groundwater planning. A comparative analysis was conducted to determine the effectiveness of the two methods in creating groundwater potential zone maps. The research cross-validated water depth data with the ROC and AUC models against the groundwater potential maps generated using both MIF and AHP methods. The results showed that

Table 12 Details results of AHP and MIF techniques

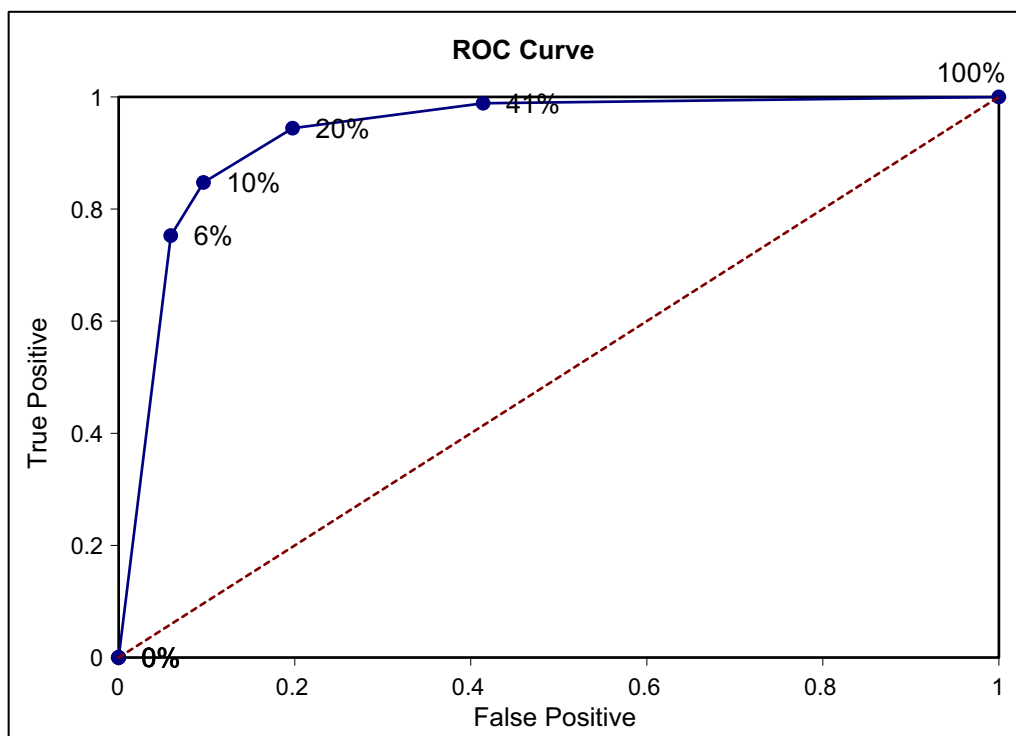| Methods	Area under different groundwater potential zones (ha) (%)				ROC and AUC models
	Poor	**Moderate**	**Good**	**Very good**	
MIF	351.29 (34.1)	511.18 (49.7)	123.95 (12.0)	41.78 (4.0)	0.80 (good)
AHP	241.50 (23.5)	285.64 (27.8)	408.31 (39.7)	92.75 (9.0)	0.93 (excellent)

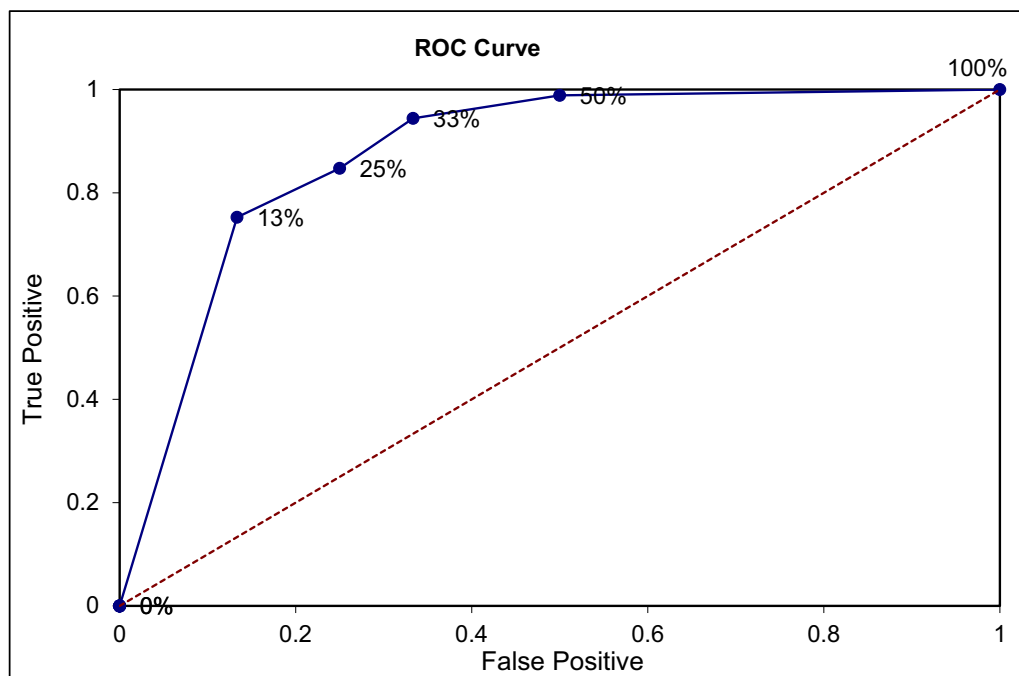**Fig. 6** Validation of GPM of AHP techniques by ROC curve

Fig. 7 Validation of GPM of MIF techniques by ROC curve

AHP had higher accuracy (0.93) in delineating potential groundwater zones compared to MIF (accuracy = 0.80). The AHP and MIF methods were evaluated using ROC curve analysis, which indicated that both methods were excellent and good for extracting groundwater potential mapping. The delineated groundwater potential maps were classified into poor, moderate, good, and very good zones. The AHP method classified the area into poor (241.50 ha), moderate (285.64 ha), good (408.31 ha), and very good (92.75 ha) zones. On the other hand, the MIF method classified the area into poor (351.29 ha), moderate (511.18 ha), good (123.95 ha), and very good (41.78 ha) zones. Based on the validation results, the MIF method identified more poor and moderate areas in the watershed than did the AHP method. All of these results are useful for sustainable planning and development of groundwater resources under climate change and for increasing the demand for fresh water, particularly in semiarid regions. RS, GIS, AHP and MIF methods and techniques can be helpful for planning and policy related to groundwater resources and aquifer management in semiarid regions. The results can be very useful for planning and developing groundwater resources, and the same methods and technology can be replicated in other areas to ensure that more beneficial results are obtained for groundwater development. The comparison analysis concluded that the combined approach of using the AHP method performed well in demarcating groundwater potential zones in the study area. The generated potential maps can be beneficial for watershed planning, soil and water conservation activities, and groundwater recharge planning in basaltic rock areas. In summary, this research demonstrated the application of the MIF and AHP methods for groundwater potential zone mapping in a watershed area. The AHP method showed higher accuracy and performed better in delineating potential groundwater zones. The findings provide valuable insights for groundwater management and planning initiatives in basaltic rock regions.

Author contributions
S.P. Shinde: Conceptualization , data creation, methodology, formal analysis, investigation, methodology, visualization, and writing—original draft. V.N. Barai: visualization, data analysis, writing review and editing and writing—original draft. B.K. Gavit: writing review. S. A. Kadam: writing review. A. A. Atre: writing review. Subodh Chandra Pal: writing review editing, formal analysis, validation. Chaitanya Baliram Pande: Conceptualization, Investigation, formal analysis, methodology writing review, writing—original draft, . Neyara Radwan: formal analysis, writing review and editing. Abebe Debele Tolche: formal analysis, writing—original draft, writing review and editing. Ismail Elkhrachy: formal analysis, writing review and editing.

Availability of data and materials

Declarations

Competing interests

The authors declare no conflict of interest.

Author details

[1]Department of Soil and Water Conservation Engineering, Dr. A.S. College of Agricultural Engineering & Technology, MPKV, Rahuri, Maharashtra, India. [2]Center for Advanced Agriculture Science and Technology on Climate-Smart Agriculture and Water Management, MPKV, Rahuri, Maharashtra, India. [3]New Era and Development in Civil Engineering Research Group, Scientific Research Center, Al-Ayen University, Thi-Qar, Nasiriyah 64001, Iraq. [4]Department of Geography, The University of Burdwan, Purba Bardhaman, West Bengal, India. [5]Department of Industrial Engineering, College of Applied Sciences, Al Maarefa University, P. O. Box 71666, 13713 Diriyah, Saudi Arabia. [6]Department of Mechanical Engineering, Faculty of Engineering, Suez Canal University, Ismailia, Egypt. [7]School of Water Resources and Environmental Engineering, Haramaya Institute of Technology, Haramaya University, P. O. Box 138, Dire Dawa, Ethiopia. [8]Civil Engineering Department, College of Engineering, Najran University, King Abdulaziz Road, 66454 Najran, Saudi Arabia.

References

1. Arabameri A, Rezaei K, Cerda A, Lombardo L, Rodrigo-Comino J (2019) GIS-based groundwater potential mapping in Shahroud plain, Iran. A comparison among statistical (bivariate and multivariate), data mining and MCDM approaches. Sci Total Environ 658:160–177. https://doi.org/10.1016/j.scitotenv.2018.12.115
2. Priyan K (2021) Issues and challenges of groundwater and surface water management in semi-arid regions. In: Pande CB, Moharir KN (eds) Groundwater resources development and planning in the semi-arid region. Springer, Cham, pp 1–17
3. Luker E, Harris LM (2019) Developing new urban water supplies: investigating motivations and barriers to groundwater use in Cape Town. Int J Water Resour Dev 35(6):917–937
4. Fathi S, Hagen JS, Matanó A, Nogueira GEH (2021) Review of GIS multi-criteria decision analysis for managed aquifer recharge in semi-arid regions. In: Pande CB, Moharir KN (eds) Groundwater resources development and planning in the semi-arid region. Springer, Cham, pp 19–52
5. Takase K, Fujihara Y (2019) Evaluation of the effects of irrigation water on groundwater budget by a hydrologic model. Paddy Water Environ 17(3):439–446
6. Kandekar VU, Pande CB, Rajesh J et al (2021) Surface water dynamics analysis based on sentinel imagery and Google Earth Engine Platform: a case study of Jayakwadi dam. Sustain Water Resour Manag 7:44. https://doi.org/10.1007/s40899-021-00527-7
7. Shiklomanov LA (1993) World freshwater resources. In: Gleick PH (ed) Water in crisis: a guide to world's freshwater resources. Oxford University Press, New York, pp 13–24
8. Zewdie MM, Kasie LA, Bogale S (2024) Groundwater potential zones delineation using GIS and AHP techniques in upper parts of Chemoga watershed. Ethiopia Appl Water Sci 14:85. https://doi.org/10.1007/s13201-024-02119-0
9. Agarwal E et al (2013) Delineation of groundwater potential zone: an AHP/ANP approach. J Earth Syst Sci 122(3):887–898
10. Asadi et al (2007) Remote sensing and GIS techniques for evaluation of groundwater quality in municipal corporation of Hyderabad (Zone-V), India. Int J Environ Res Public Health 4(1):45–52
11. Shailaja G, Kadam AK, Gupta G, Umrikar BN, Pawar NJ (2019) Integrated geophysical, geospatial and multiple-criteria decision analysis techniques for delineation of groundwater potential zones in a semi-arid hard-rock aquifer in Maharashtra, India. Hydrogeol J 27(2):639–654
12. Qadir J, Bhat MS, Alam A, Rashid I (2019) Mapping groundwater potential zones using remote sensing and GIS approach in Jammu Himalaya Jammu and Kashmir. Geo-Journal 85(2):487–504
13. Gueretz JS, Da Silva FA, Simionatto EL, Férard JF, Radetski CM, Somensi CA (2020) A multi-parametric study of the interaction between the Parati river and Babitonga Bay in terms of water quality. J Environ Sci Health Part B 55:257–264
14. Mahato S, Pal S (2018) Changing land surface temperature of a rural Rarh tract river basin of India. Remote Sens Appl Soc Environ 10:209–223
15. Pande CB, Moharir KN, Khadri SFR et al (2018) Study of land use classification in an arid region using multispectral satellite images. Appl Water Sci 8:123
16. Ghimire M, Chapagain PS, Shrestha S (2019) Mapping of groundwater spring potential zone using geospatial techniques in the central Nepal Himalayas: a case example of Melamchi-Larke area. J Earth Syst Sci 128(2):26
17. Rajesh J, Pande CB, Kadam SA (2021) Exploration of groundwater potential zones using analytical hierarchical process (AHP) approach in the Godavari river basin of Maharashtra in India. Appl Water Sci 11:182. https://doi.org/10.1007/s13201-021-01518-x
18. Pande CB, Moharir KN, Panneerselvam B et al (2021) Delineation of groundwater potential zones for sustainable development and planning using analytical hierarchy process (AHP), and MIF techniques. Appl Water Sci 11:186. https://doi.org/10.1007/s13201-021-01522-1
19. Selvarani AG, Elangovan K, Kumar CS (2016) Evaluation of groundwater potential zones using electrical resistivity and GIS in Noyyal River basin Tamil Nadu. J Geol Soc India 87(5):573–582. https://doi.org/10.1007/s12594-016-0431-8
20. Murmu P, Kumar M, Lal D, Sonker I, Singh SK (2019) Delineation of groundwater potential zones using geospatial techniques and analytical hierarchy process in Dumka district, Jharkhand India. Groundw Sustain Dev 9:100239. https://doi.org/10.1016/j.gsd.2019.100239
21. Pande CB, Moharir KN, Singh SK et al (2022) Groundwater flow modeling in the basaltic hard rock area of Maharashtra, India. Appl Water Sci 12:12. https://doi.org/10.1007/s13201-021-01525-y
22. Pande CB, Moharir KN, Singh SK, Varade AM (2019) An integrated approach to delineate the groundwater potential zones in Devdari watershed area of Akola district, Maharashtra, Central India. Environ Dev Sustain 22:4867
23. Magesh NS, Chandrasekar N, Soundranayagam JP (2012) Delineation of groundwater potential zones in Theni district, Tamil Nadu, using remote sensing. GIS MIF Tech Geosci Front 3(2):189–196
24. Kahneman D (2011) Thinking, fast and slow. Farrar Straus and Giroux, New York
25. Mu E, Pereyra-Rojas M (2016) AHP models with sub-criteria. In: Springer briefs in operations research, Springer, Cham, pp 45–56. https://doi.org/10.1007/978-3-319-33861-3_4
26. Saaty TL (1980) The analytical hierarchy process. McGraw Hill, New York
27. Saaty TL (1986) Axiomatic foundation of the analytic hierarchy process. Manage Sci 32:841–855
28. Saaty TL (1990) How to make a decision: the analytic hierarchy process. Eur J Oper Res 48:9–26
29. Saaty TL (2008) Decision making with the analytic hierarchy process. Int J Serv Sci 1(1):83–98
30. Ghosh KP, Bandyopadhyay S, Jana NC (2015) Mapping of groundwater potential zones in hard rock terrain using geoinformatics: a case of Kumari watershed in western part of West Bengal. Model Earth Syst Environ 2:1
31. Manap MA, Nampak H, Pradhan B, Lee S, Sulaiman WNA, Ramli MF (2014) Application of probabilistic-based frequency ratio model in groundwater potential mapping using remote sensing data and GIS. Arab J Geosci 7(2):711–724
32. Pourtaghi ZS, Pourghasemi HR (2014) GIS-based groundwater spring potential assessment and mapping in the Birjand Township, southern Khorasan Province, Iran. Hydrogeol J 22:643–662. https://doi.org/10.1007/s10040-013-1089-6
33. Ozdemir A (2011) GIS-based groundwater spring potential mapping in the Sultan Mountains (Konya, Turkey) using frequency ratio, weights of evidence and logistic regression methods and their comparison. J Hydrol 411(3–4):290–308

Shinde *et al. Environmental Sciences Europe*   (2024) 36:87

Page 20 of 20

34. Pourghasemi HR, Pradhan B, Gokceoglu C (2012) Application of fuzzy logic and analytical hierarchy process (AHP) to landslide susceptibility mapping at Haraz watershed, Iran. Nat Hazards 63(2):965–996. https://doi.org/10.1007/s11069-012-0217-2

35. Khadri SFR, Pande C, Moharir K (2013) Geomorphological investigation of WRV-1 watershed management in Wardha district of Maharashtra India; using remote sensing and geographic information system techniques. Int J Pure Appl Res Eng Technol 1(10):18–35

36. Khadri SFR, Pande C (2015) Remote sensing based hydro-geomorphological mapping of Mahesh River Basin Akola and Buldhana Districts, Maharashtra, India-effects for water resource evaluation and management. Int J Geol Earth Environ Sci 5(2):178–187

37. Bera K, Bandyopadhyay J (2012) Ground water potential mapping in Dulung watershed using remote sensing and GIS techniques West Bengal, India. Int J Scientifc Res Publ 2(12):1–7

38. Li Y, Xiao J, Wang Y, Deng C (2022) Numerical simulation investigation on fracture propagation of fracturing for crossing coal seam roof. Processes 10(7):1296. https://doi.org/10.3390/pr10071296

39. Ma D, Li Q, Cai Kc et al (2023) Understanding water inrush hazard of weak geological structure in deep mine engineering: a seepage-induced erosion model considering tortuosity. J Cent South Univ 30:517–529. https://doi.org/10.1007/s11771-023-5261-4

40. Li R, Zhu G, Lu S, Sang L, Meng G, Chen L et al (2023) Effects of urbanization on the water cycle in the Shiyang River basin: based on a stable isotope method. Hydrol Earth Syst Sci 27(24):4437–4452. https://doi.org/10.5194/hess-27-4437-2023

41. Zhu G, Yong L, Zhao X, Liu Y, Zhang Z, Xu Y et al (2022) Evaporation, infiltration and storage of soil water in different vegetation zones in the Qilian Mountains: a stable isotope perspective. Hydrol Earth Syst Sci 26(14):3771–3784. https://doi.org/10.5194/hess-26-3771-2022

42. Dai H, Liu Y, Guadagnini A, Yuan S, Yang J et al (2024a) Comparative assessment of two global sensitivity approaches considering model and parameter uncertainty. Water Resourc Res 60(2):e2023WR036096. https://doi.org/10.1029/2023WR036096

43. Dai H, Ju J, Gui D, Zhu Y, Ye M, Liu Y at al (2024b) A two-step Bayesian network-based process sensitivity analysis for complex nitrogen reactive transport modeling. J Hydrol 632:130903. https://doi.org/10.1016/j.jhydrol.2024.130903

44. Huang J, Gómez-Dans JL, Huang H, Ma H, Wu Q, Lewis PE et al (2019) Assimilation of remote sensing into crop growth models: current status and perspectives. Agricult Forest Meteorol 276–277:107609. https://doi.org/10.1016/j.agrformet.2019.06.008

45. Guan H, Huang J, Li L, Li X, Miao S, Su W et al (2023) Improved Gaussian mixture model to map the flooded crops of VV and VH polarization data. Remote Sens Environ 295:113714. https://doi.org/10.1016/j.rse.2023.113714

46. Li Q, Lu L, Zhao Q, Hu S (2023) Impact of inorganic solutes' release in groundwater during oil shale in situ exploitation. Water 15(1):172. https://doi.org/10.3390/w15010172

47. Zhang K, Li Y, Yu Z, Yang T, Xu J, Chao L et al (2021) Xin'anjiang nested experimental watershed (XAJ-NEW) for understanding multiscale water cycle: scientific objectives and experimental design. Engineering 18(11):207–217. https://doi.org/10.1016/j.eng.2021.08.026

48. Chen G, Zhang K, Wang S, Xia Y, Chao L (2023) iHydroSlide3D v1.0: an advanced hydrological–geotechnical model for hydrological simulation and three-dimensional landslide prediction. Geosci Model Dev 16(10):2915–2937. https://doi.org/10.5194/gmd-16-2915-2023

49. Zhao Y, Wang H, Song B, Xue P, Zhang W, Peth S et al (2023) Characterizing uncertainty in process-based hydraulic modeling, exemplified in a semiarid inner Mongolia steppe. Geoderma 440:116713. https://doi.org/10.1016/j.geoderma.2023.116713

50. Yi J, Li H, Zhao Y, Shao M, Zhang H, et al (2022) Assessing soil water balance to optimize irrigation schedules of flood-irrigated maize fields with different cultivation histories in the arid region. Agricult Water Manag 265:107543. https://doi.org/10.1016/j.agwat.2022.107543

51. Zhang T, Song B, Han G, Zhao H, Hu Q, Zhao Y et al (2023) Effects of coastal wetland reclamation on soil organic carbon, total nitrogen, and total phosphorus in China: A meta-analysis. Land Degrad Develop 34(11):3340–3349. https://doi.org/10.1002/ldr.4687

52. Jiang C, Wang Y, Yang Z, Zhao Y (2023) Do adaptive policy adjustments deliver ecosystem-agriculture-economy co-benefits in land degradation neutrality efforts? Evidence from southeast coast of China. Environ Monit Assess 195(10):1215. https://doi.org/10.1007/s10661-023-11821-6

53. Yang M, Wang H, Hu K, Yin G, Wei Z (2022) IA-Net: an inception–attention-module-based network for classifying underwater images from others. IEEE J Oceanic Eng 47(3):704–717. https://doi.org/10.1109/JOE.2021.3126090

54. Xu J, Zhou G, Su S, Cao Q, Tian Z (2022) The development of a rigorous model for bathymetric mapping from multispectral satellite-images. Remote Sens 14(10):2495. https://doi.org/10.3390/rs14102495

55. Zhou G, Liu X (2022) Orthorectification model for extra-length linear array imagery. IEEE Trans Geosci Remote Sens 60:4709710. https://doi.org/10.1109/TGRS.2022.3223911

56. Zhou G, Li H, Song R, Wang Q, Xu J et al (2022) Orthorectification of fisheye image under equidistant projection model. Remote Sens 14(17):4175. https://doi.org/10.3390/rs14174175

57. Wu Z, Zhu H, He L, Zhao Q, Shi J et al (2023) Real-time stereo matching with high accuracy via spatial attention-guided upsampling. Appl Intell 53(20):24253–24274. https://doi.org/10.1007/s10489-023-04646-w

58. Peng JJ, Chen XG, Wang XK, Wang JQ, Long QQ et al (2023) Picture fuzzy decision-making theories and methodologies: a systematic review. Int J Syst Sci 54(13):2663–2675. https://doi.org/10.1080/00207721.2023.2241961

59. Li J, Pang Z, Liu Y, Hu S, Jiang W, Tian L et al (2023) Changes in groundwater dynamics and geochemical evolution induced by drainage reorganization: evidence from 81Kr and 36Cl dating of geothermal water in the Weihe Basin of China. Earth Planet Sci Lett 623:118425. https://doi.org/10.1016/j.epsl.2023.118425

60. Yin L, Wang L, Li T, Lu S, Yin Z, Liu X et al (2023) U-Net-STN: a novel end-to-end lake boundary prediction model. Land 12(8):1602. https://doi.org/10.3390/land12081602

61. Yin L, Wang L, Keim BD, Konsoer K, Yin Z, Liu M et al (2023) Spatial and wavelet analysis of precipitation and river discharge during operation of the three gorges dam, China. Ecol Ind 154:110837. https://doi.org/10.1016/j.ecolind.2023.110837

62. Yin L, Wang L, Li T, Lu S, Tian J, Yin Z et al (2023) U-Net-LSTM: time series-enhanced lake boundary prediction model. Land 12(10):1859. https://doi.org/10.3390/land12101859

63. Pande CB, Moharir KN, Singh SK, Varade AM, Elbeltagi A, Khadri SFR, Choudhari P (2021) Estimation of crop and forest biomass resources in a semi-arid region using satellite data and GIS. J Saudi Soc Agric Sci 20(5):302–311. https://doi.org/10.1016/j.jssas.2021.03.002

64. Moharir KN, Pande CB, Gautam VK, Singh SK, Rane NL (2023) Integration of hydrogeological data, GIS and AHP techniques applied to delineate groundwater potential zones in sandstone, limestone and shales rocks of the Damoh district, (MP) central India. Environ Res 228:115832

65. Pande CB, Al-Ansari N, Kushwaha NL, Srivastava A, Noor R, Kumar M, Moharir KN, Elbeltagi A (2022) Forecasting of SPI and meteorological drought based on the artificial neural network and M5P model tree. Land 11(11):2040. https://doi.org/10.3390/land11112040

66. Gautam VK, Pande CB, Kothari M, Singh PK, Agrawal A (2022) Exploration of groundwater potential zones mapping for hard rock region in the Jakham river basin using geospatial techniques and aquifer parameters. Adv Space Res 71:2892–2908. https://doi.org/10.1016/j.asr.2022.11.022

Publisher's Note